Journal of Material and Process Technologies

Available online at http://journal.aastu.edu.et/

Magnetically Recyclable Activated Carbon Prepared from Brewer's Spent Grain and Its Chromium (VI) Adsorption Study

Belay Getye [1,2], Gebrehiwot Gebreslassie[1,2],Tsegaye Sissay Tedla[3,4], Getachew Adam Workneh[1,3]*

[1]*Department of Industrial Chemistry, Addis Ababa Science and Technology University, P.O.Box 16417, Addis Ababa, Ethiopia*
[2]*Nanotechnology Center of Excellence, Addis Ababa Science and Technology University, P.O.Box 16417, Addis Ababa, Ethiopia*
[3]*Sustainable Energy Center of Excellence, Addis Ababa Science and Technology University, P.O.Box 16417, Addis Ababa, Ethiopia*
[4]*Department of Chemical Engineering, Addis Ababa Science and Technology University, P.O.Box 16417, Addis Ababa, Ethiopia*

Article Information

Article history:
Received 6 Nov 2024
Received in revised form 28 Dec 2024
Accepted 28 Dec 2024

Keywords:
Brewery spent grain,
Magnetic Activated Carbon,
Adsorption,
Chromium (VI)

*Corresponding author.
E-mail: getachew.adam@aastu.edu.et
(Getachew Adam Workneh)

https://doi.org/10.69660/jmpt.v1i2.83

Abstract

Magnetic Activated carbon was prepared from a brewery spent grain (BSG) and magnetite using the sol-gel method. The crystal structure, molecular constituent, morphology, and specific surface area of the prepared magnetic activated carbon (MAC) were analyzed using XRD, FTIR, SEM, and BET techniques. The characterization results revealed the successful preparation of MAC material. The removal efficiency of MAC for Cr (VI) from synthetic wastewater and real wastewater was investigated. The adsorption process was optimized numerically and found that solution pH of 2, initial concentration of 40 mg L^{-1}, an adsorbent dosage of 5 g L^{-1}, and a contact time of 30 min were the optimal conditions for removal of Cr (VI) with 97.5% efficacy. The adsorption studies were consistent with the pseudo-second-order kinetics and with Temkin isotherm models with a high regression coefficient (R^2) of 0.995 and 0.996 respectively. Moreover, at the optimum conditions, the MAC adsorbent showed the removal of 318 ± 14 mg/L chemical oxygen demand (COD), and 41.3±7.8 mgL^{-1} biochemical oxygen demand (BOD) of real wastewater collected from the local tannery industry in Ethiopia. Furthermore, the recycled MAC was used repeatedly and showed comparable removal efficiency for five consecutive cycles. As such, magnetic activated carbon made from BSG was found as an alternative efficient adsorbent in tannery wastewater treatment.

1. Introduction

Contamination of the environment by persistent pollutants from different activities has become an increasingly severe problem [1], [2]. It has increased exponentially in the past few years and reached an alarming level in terms of its effects on living creatures. Particularly, the disposal of untreated wastewater containing heavy metals has a harmful impact on the ecosystem and human health [2] – [4]. For instance, heavy metals such as Cr(VI) are the major ions produced in large volumes in different industrial activities as these metals cannot be degraded easily [5]–[7]. Therefore, removal of the Cr (VI) from the wastewater effluent before releasing it into the environment is paramount to overwhelming the environmental problem. There are various methods to eliminate Cr(VI) from wastewater such as ion exchange, ultrafiltration, chemical precipitation, electrochemical oxidation, coagulation-flocculation, adsorption, and so on [8]–[10]. However, some of these approaches are costly, use dangerous chemicals, and generate toxic sludge as a byproduct which is harmful to the environment and people. Among the above-mentioned methods, adsorption is considered as a promising technique due to its simplicity of design, and easy operation [11]. Then again, activated carbon (AC) is the most widely used adsorbent due to its large surface area, porosity, high adsorption capacity, and low cost. As a result, AC has become an excellent and well-known adsorbent for heavy metal removal from industrial wastewater [12]. Though AC shows outstanding removal performance of heavy metals, the difficulty of AC separation from solution significantly affects its practical application. Fe_3O_4 has been widely used to synthesize magnetic activated carbon to achieve the characteristics of easy separation of activated carbon. For instance, Parlayici et. al. reported magnetic Fe_3O_4/activated carbon for the removal of heavy metals [13]. Inappropriately, most reported MAC materials usually showed poor stability, so designing and preparing a novel magnetic carbon composite adsorbent with good stability is still required.

In this work, magnetic activated carbon (MAC) has been synthesized from brewery spent grain and Fe_3O_4. The crystallinity, molecular structure, surface morphology, and surface area of the prepared MAC were characterized using X-Ray diffraction (XRD), Fourier Transform Infrared Spectroscopy (FTIR), Scanning electron microscope (SEM), and Brunauer, Emmett and Teller (BET) characterization techniques. Then, the adsorption efficiency and mechanism of MAC for Cr (VI) from simulated and real wastewater were studied.

2. Experimental Part

2.1. Chemicals and Materials

Tamarind indica fruit was collected from a local Dire Dawa, Kefira market trader. The fruits were taken to the Addis Ababa Science and Technology Food Science and Applied Nutrition Laboratory for further analysis. Tamarind indica were sorted to remove dirt and bad fruits. After removing the dirt, the tamarind fruit was washed and the raw tamarind fruit was soaked and roasted for analysis.

2.2. Preparation of activated carbon

The brewery spent grain (BSG) sample was collected from Heineken Brewery Share Company (HBSC), Addis Ababa, Ethiopia. The BSG was then washed repetitively many times with distilled water to remove impurities and dried in the oven at 60 0C for 24 hrs. Then, the dried BSG was ground, and sieved by 250 μm sieve. Thereafter, 60 g BSG were transferred into conical flasks containing 50% (wt.) H3PO4 concentrations and covered with aluminum foil and left over for 24 hrs.[14]. Afterwards, the treated sample was washed thoroughly with distilled water, and transferred into crucibles and dried at 105 0C in oven for 24 hrs. The carbonization process of the dried samples was initiated at 200 0C for 30 min, and further carbonization process was made at 500 0C for 2 hrs. After the sample was allowed to cool to room temperature, the prepared AC was washed repeatedly with hot distilled water to remove all the excess acid until the pH of the filtrate was approximately 7. Finally, prepared AC was dried at 105 0C for 24 h and labeled as AC-500, and kept in a desiccator for further analysis.

2.3. Preparation of magnetic activated carbon

MAC was prepared from AC, $FeCl_3.6H_2O$ and $FeCl_2.4H_2O$. First, 6 g AC was dissolved in 200 ml distilled water in 500 mL beaker (Solution A). Then, 3 g of $FeCl_3.6H_2O$ dissolved in 100 ml distilled and 1.5 g of $FeCl_2.4H_2O$ dissolved in 50 ml distilled water were mixed in 200 ml beaker (Solution B). Thereafter, solution A and solution B were mixed in 500 ml beaker and stirred for 1 hrs. [11]. Subsequently, the pH of the mixed solution was adjusted to pH of 11 by adding 0.1M of NaOH aqueous solution dropwise and heated to a temperature of 70 ℃ with vigorous stirring using magnetic stirrer. Then, after cooling to room temperature and aging for 24 hrs, the produced MAC was separated using magnet and washed using distilled water and ethanol. Finally, the prepared MAC was labeled and dried at 50 ℃ in an oven overnight.

2.4. MAC Characterization

The crystalline structure of the prepared sample was studied using an XRD (Pan Analytical X'PRO MRD X-ray diffractometer) equipped with Cu K α - radiation (λ = 1.5406 Å) in 2θ range of 10 to 80° continuously with a step of 0.013° and 30.35 seconds /step. The operating voltage and current were 40 kV and 30 mA, respectively at ambient temperature [15]. The morphology of MAC was examined using SEM (INSPCT-F50, FEI) operated at an accelerating voltage of 20 kV. The specific surface area of the sample was calculated from N2 adsorption–desorption isotherms measured using BET surface area analyzer (SA-9600 series, Horiba) [16]. The functional groups on the surface of the MAC was examined using FT-IR (PerkinElmer, USA) in a spectral range of 400 - 4000 cm^{-1}[17].

2.5. Effect of Process Variables and Multivariate Design of Experiment

The experimental data were investigated using Design Expert software (version 12). Response surface methodology-central composite design (RSM-CCD), an extensively used statistical technique tool on the multivariate nonlinear. RSM is a set of statistical and mathematical method which is helpful in creating empirical models, refining and optimizing process parameters, and determining how various influencing factors interact [18]. Four independent variables such as dosage (A), contact time (B), pH (C) and initial metal ion concentration (D) were considered in this study. The interaction effect of four factors and the consequence they have on the adsorption percentage removal of Cr (VI) had been studied using CCD by setting four levels for each of the parameters (Table 1). The adsorption process was opimized numerical by RSM which involves three major steps. These are performing the statistically designed experiments, estimating the coefficients in a mathematical model and predicting the response and checking the adequacy of the model [19]. RSM-CCD was applied to model and optimize different process parameters of adsorption capacity of MAC. A total of 30 experimental run with twenty-four unique experimental conditions and six central replicates were carried out as generated by design expert software.

Using a second-degree polynomial equation, the response was utilized to create an empirical model that correlates to the experimental variables (equation (1)).

$$y = \beta_0 + \sum_{i=1}^{n} \beta_i X_i + \sum_{i=1}^{n} \beta_{ii} x^2{}_i + \sum_{i}^{n} \sum_{j=i+1}^{n} \beta_{ij} X_i X_j + \xi \quad (1)$$

Where y is the response variable, β_0 is the constant, β_i is the linear cofficients, β_{ii} is the quadratic coefficents, β_{ij} is the interaction coefficients, x_i and x_j are the coded variable parameters, n is number of factors and ξ is the rondom errors. The factors with the corresponfing coded factors are shown in Table 1. To determine the interaction between the process variables and the responses and to estimate the statistical parameters, graphical analyses of the data have been performed using ANOVA (Analysis of Variance). The coefficient of determinations (R^2) provided an estimate of the fitted polynomial model accuracy. The 95% confidence interval probability value (P-value) was used to assess the significant model terms.

Table 1. Parameters and corresponding levels for RSM-CCD experiments.

Parameters	Factor code	Unit	Lower limit	Upper limit
Dosage	A	gmL^{-1}	3	7
time	B	min	20	40
pH	C	-	1	3
Initial concentration	D	mgL^{-1}	20	60

2.6. Batch Adsorption Experiment

Batch adsorption studies were conducted at room temperature. For the adsorption of Cr (VI) on MAC, different doses of MAC (0.1 - 2 g) were added to 100 ml solution initially containing 20 to 120 mg L-1 of Cr (VI) solutions. The pH of Cr (VI) solutions was adjusted into pH values of 2–6 using 0.1 M NaOH and HCl solution. Each mixture was agitated for 10, 30, 50, 70 and 90 min at 200 rpm in an orbital shaker. After the adsorption was allowed to take place and aged, the solution from the shaker was filtered. The concentration of Cr (VI) in solution was measured using UV–Visible spectrophotometer (Biochrom Libra S50, United Kingdom) at λ = 540 nm after reacted with 1,5-diphenyl carbazide 0.25% w/v in acetone and 0.2 N sulfuric acid. The percentage removal and the adsorption capacity were calculated according to equation (2) and (3), respectively.

$$R(\%) = \frac{C_o - C_f}{C_o} \times 100 \quad (2)$$

$$q = \frac{(C_o - C_f)V}{m} \quad (3)$$

Where C_o (mgL^{-1}) is the initial concentration of Cr (VI), C_f (mgL^{-1}) is the final concentration of Cr(VI) after batch adsorption, q (mgL^{-1}) is the amount of Cr (VI) adsorbed by the adsorbent, V(L) is the volume of Cr(VI) solution, and m (g) is the mass of adsorbent.

Adsorption study on real waste water: Wastewater was collected from a local leather factory (Pittards Ethiopia Tannery S.C.) located at Addis Ababa, Ethiopia and its pH, DO, BOD, COD, TSS and TDS values were examined before and after batch adsorption. The amount of Cr (VI) concentration in the real wastewater before and after adsorption was analyzed by double beam UV-VIS spectrophotometer (Biochrom Libra S50, United Kingdom) by following a standard procedure [20].

2.7. Adsorption isotherm and kinetics study

Adsorption Isotherm Study: The equilibrium isotherms were studied by taking 200 mL of Cr (VI) solutions at different initial concentrations of 20 - 100 mg L^{-1} in 250 mL Erlenmeyer flasks and pH solution was adjusted to 2. A 0.5 g of MAC was added to the solutions and agitated at 200 rpm for 30 min. To establish the adsorptions capacity of MAC experimental data was fitted against model isotherm equations of Langmuir, Freundlich and Temkin [21].

Kinetic Study: Kinetic study was conducted by taking 200 ml of Cr (VI) solutions with initial concentrations of 40 mg L^{-1} in 250 ml Erlenmeyer flasks and adjusting the pH to 2. Then 0.5 g of MAC was added and the solution was agitated at 200 rpm. Solutions were sampled at a time interval of (10 - 80 min) and the filtrate was analyzed for the remaining Cr (VI) concentration. The kinetics of Cr (VI) adsorptions on MAC were analyzed using pseudo first-order and pseudo second-order kinetic models [22].

2.8. Recyclability Study of MAC adsorbent

Recyclability and stability of the MAC adsorbent were studied following the same procedure with the batch adsorption but using the adsorbent repeatedly for consecutive batch adsorption.

3. Results and discussion

3.1. Characterization of AC and MAC adsorbents

Physicochemical analysis: Physicochemical properties of the prepared AC and MAC were studied and the results shows ash content is higher in AC than in MAC (Table 2). Moreover, the fixed carbon percentage of AC (64.29%) is less than the fixed carbon percentage of MAC (74.4%). The lower ash content and volatile matters in MAC are attributed to lower inorganic content and higher fixed carbon. Therefore, higher value of fixed carbon in MAC shows, the MAC adsorbent is having more efficiency and stability than that of AC adsorbent [23].

Table 2: Physio-chemical characteristics of AC and MAC

Physio-chemical properties	AC	MAC
Moisture Content (%)	5.13	5.51
Volatile Content (%)	22.93	18
Ash content (%)	7.6	5.1
Fixed Carbon (%)	64.29	71.4
pH	6.7	6.5

XRD analysis: The crystalline structure of MAC was investigated using XRD and the result is presented in Figure 1(a). As can be seen from the XRD pattern in Figure 1(a), the peaks at 2θ value of 18.26, 30, 35, 43.24, 53.46, 57.12, and 62.56° were recognized as the (220), (311), (400), (422), (511), (440) and (622) planes of face-centered cubic structure of Fe_3O_4 [24]. Also, the peak at 2θ value of 24° corresponds to the amorphous carbon [25]. Therefore, the prepared MAC contains minerals of graphite and magnetite. No other peak is detected ascribed to impurities or other residuals in the fabricated sample structure. Furthermore, the average particle size of Fe_3O_4 was calculated using Scherrer equation from the diffraction peak (311) and the value was found to be 22 nm.

FTIR Analysis: The FTIR spectra of MAC was displayed in Figure 1(b). The peak at 3667 cm^{-1} represents $^{-}$OH stretching vibration. The bands in the 2981, 2901, 1398 and 1239 cm^{-1} are characteristics of the stretching vibration and the flexural vibration of C-H. The intense peak positioned at 1050 cm^{-1} could be assigned to C-O vibrations in secondary and primary R–OH groups in alcohols [26]. The small bands at 881 cm^{-1} were attributed to the out-of-plane bending vibrations of C-H in benzene derivatives. Furthermore, the peak at 543 cm^{-1} is due to the formation of Fe-O [27].

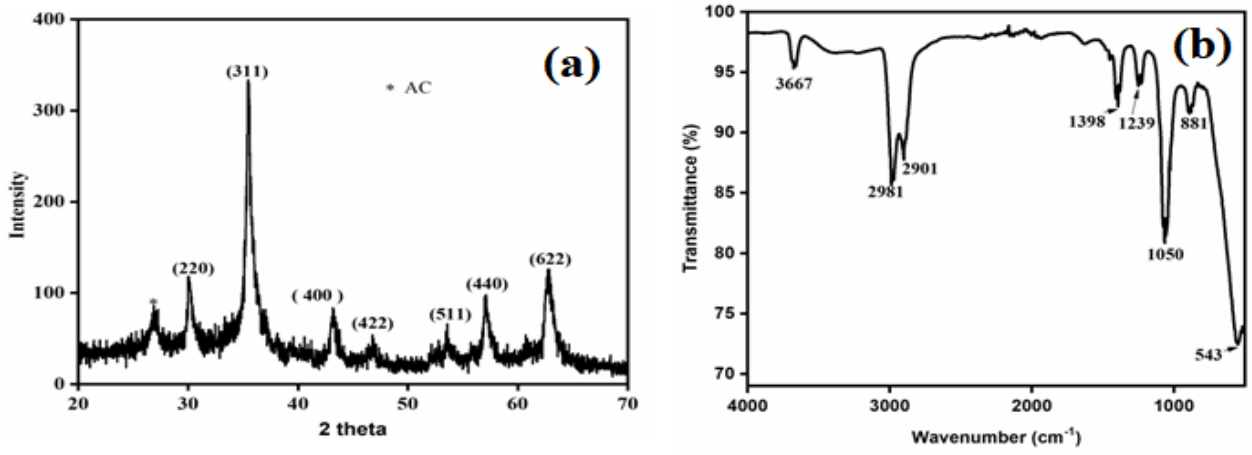

Figure 1: (a) XRD analysis of MAC and (b) FT-IR spectra of MAC.

BET Analysis: Textural properties of AC and MAC adsorbents were studied using N_2 adsorption-desorption technique. The specific surface area of AC and MAC materials were found to be 695 m^2/g and 494 m^2/g, respectively. Thus, the surface area of AC is greater than that of MAC. This

might be due to the coverage of some parts of AC by Fe_3O_4 nanoparticles in the MAC (AC/Fe_3O_4) adsorbent [4].

SEM Analysis: The morphology of the AC and MAC were examined by SEM images as displayed in Figure 2 (a & b). As shown in Figure 2 (a), the typical sheet-like porous structure of AC were observed while in Figure 2(b), a relatively dense structure which might be due to the loaded Fe_3O_4 nanoparticles on the surface of AC sheet is observed, suggesting the formation AC/Fe_3O_4 (AC/MAC) nanocomposite. Comparing the two images, the AC (Figure 2(a)) was more porous than the MAC (Figure 2(b)). This result is consistent with the BET analysis.

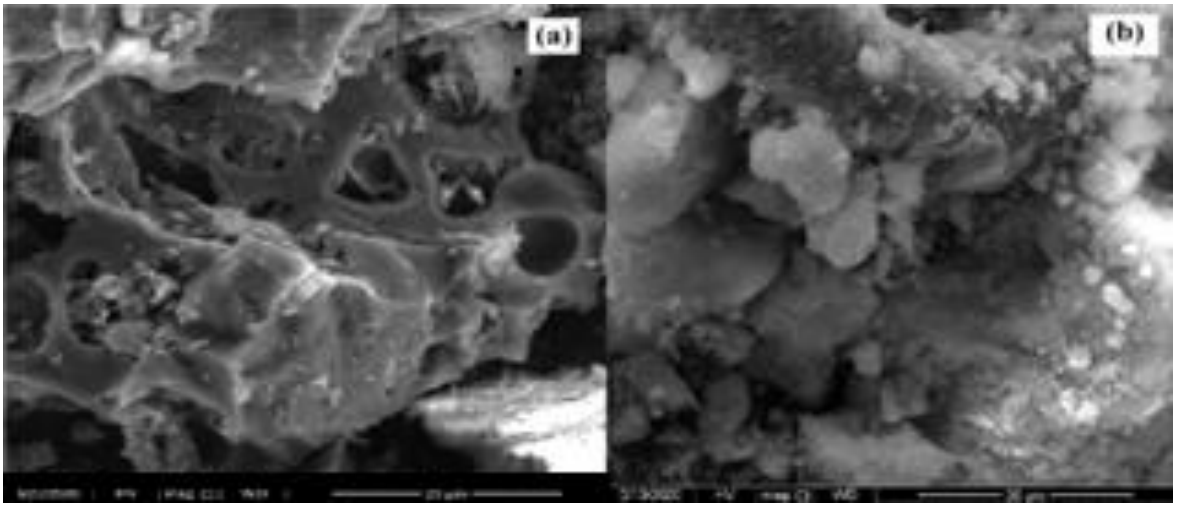

Figure 1: SEM image of (a) AC, and (b) MAC adsorbents.

3.2. Optimization and Effect of Parameters

3.2.1. Individual parameter effect

Effect of contact time: The effect of contact time on the removal efficiency of the MAC adsorbent at constant pH of 2, initial Cr (VI) concentration of 40 mg L^{-1} and dosage of MAC = 5 g L^{-1} is shown in Figure 3 (a). As the adsorption time increased from 10 to 30 min, the removal capacity of the MAC was increased rapidly from 55% to 97 %. Due to the availability of many free active sites on the adsorbent surface, an increase in the removal efficiency was observed up to 30 min. However, the removal capability of MAC was almost constant above 30 min. This may be due to adsorption process reaching at equilibrium point. As a result, the optimum time was found to be 30 min.

Effect of pH: The effect of pH on the removal efficiency of MAC was examined and optimized by varying the pH from pH 1 to 6 by keeping the MAC dose, contact time, and initial concentration of Cr (VI) to 5g L^{-1}, 40 mg L^{-1}, and 30 min, respectively constant. As presented in Figure 3(b), the removal efficiency of MAC was found to be higher at low pH values. As the pH increased from pH 1 to 2, the removal efficiency slightly increased. On the other hand, as the pH increased from pH 2 to 6, the percent removal gradually decreased from 96.6% to 48%. Therefore, the optimum pH was found to be pH 2. This is consistent with other literature findings [28].

Effect of initial Cr (VI) concentration: The effect of initial Cr (VI) concentration was optimized by varying from 20 mg L^{-1} to 120 mg L^{-1} keeping the pH 2, contact time 30 min, and dose of MAC 5 mg L-1 constant. As initial concentration increased from 20 mg/L to 40 mg/L, the removal ability of MAC was remained constant (97.5%) (Figure 3(c)). Increasing the initial concentration above 40 mg L^{-1}, diminished the removal capacity to 48.3% which might be due to the saturation of active sites of MAC with more Cr (VI) ions in the solution. So, the optimum initial concentration was found to be 40 mg L^{-1}.

Effect of adsorbent dose: Keeping all the other parameters constant, as the MAC adsorbent dose increased from 1g L^{-1} to 5g L^{-1}, the removal efficiency increased from 71 to 95% as shown in Figure 3(d). This increment in percentage removal of Cr (VI) is due to the increment of active sites of adsorbent to adsorb the pollutant. Then again, for the adsorbent dosage above 5g L^{-1}, the removal efficiency remains almost the same. Because as the adsorbent dose increases aggregation of particles happens and a number of active sites may not be increased. Therefore, the optimum dose is then 5 g L^{-1}, with 95% removal efficiency of Cr (VI) ions from simulated wastewater.

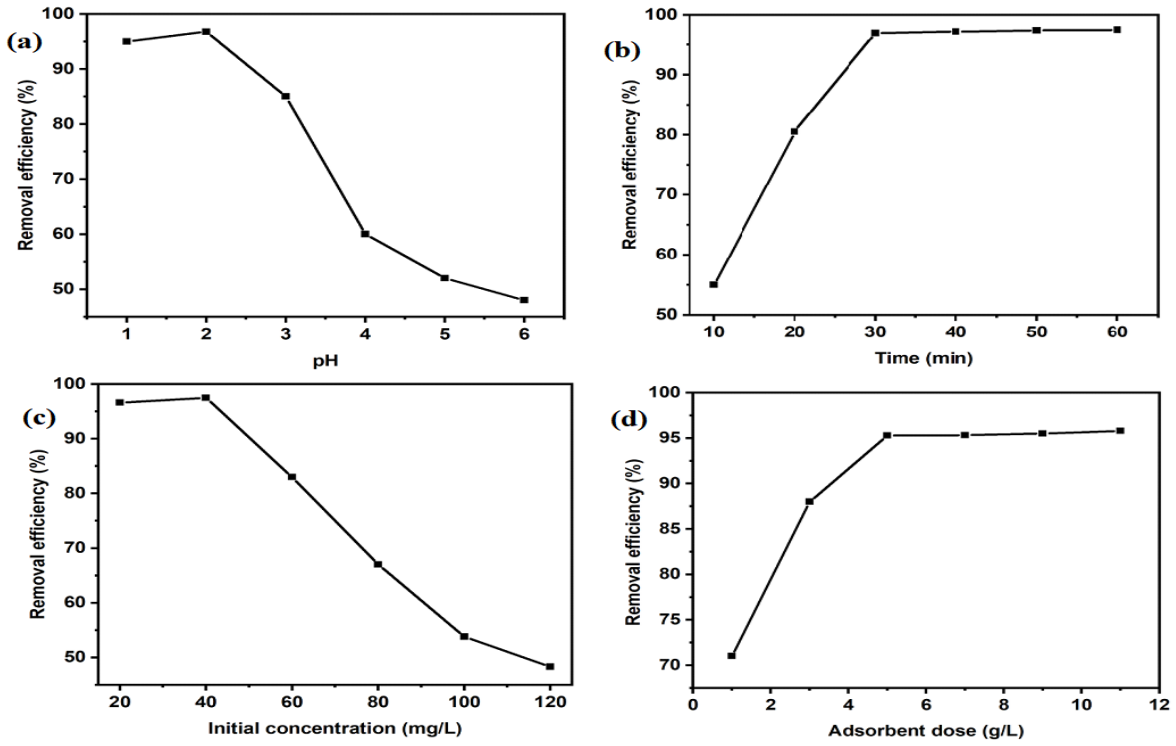

Figure 2: (a) The effect of contact time, **(**b**)** effect of pH, **(c)** effect of initial concentration, **(**d) effect of MAC dosage on the Chromium (VI) removal.

3.2.2. Interaction effect of adsorption factors

The key objective of CCD method applied in this study was to find out the substantial effects of the process parameters such as initial concentration, pH, adsorbent dose and contact time on the removal efficiency of Cr (VI). Three-dimensional (3D) response surface plots were used to investigate the effect of all the factors on the responses (Figure 4 (a-f)).

Effect of dosage and contact time: The interaction effect of adsorbent dose and contact time on the percent removal of Cr (VI) is presented in Figure 4(a). Maximum Cr (VI) removal was obtained at adsorbent dose range of 3 to 5 g L^{-1}. The removal of Cr (VI) increased with the rise of the adsorbent amount up to a certain level and further increasing contact time resulted in the increment of percent removal of Cr (VI). The maximum removal efficiency, which is 96.55%, as can be observed from Figure 4(a), is at the intersection point of 5 g L^{-1} adsorbent dosage and 30 min contact time.

Effect of dosage and pH: The interaction between pH and adsorbent dose on Cr (VI) removal is displayed in Figure 4 (b). It was noticed that a direct decrease in the Cr (VI) ion removal occurred when the pH value of the solutions changed from 1 to 3. The maximum removal of Cr (VI) ions is found at pH 2. The decrease in Cr (VI) ion removal efficiency at higher pH might be due to the competition between OH- and chromate ions (CrO_4^{2-}), where the former being the dominant species wins the race. Conversely, the increment in the adsorbent dose increases the removal efficiency of Cr (VI) and the maximum removal efficiency was found at a dose between 3 to 5 g L^{-1}. The highest value of removal efficiency (96.5%) is observed for the values of dosage 5g L^{-1} and pH 2.

Effect of dosage and initial concentration: The interaction effect of initial Cr (VI) concentration and adsorbent dose on the percentage removal of chromium (VI) is revealed in Figure 4(c). The initial Cr (VI) concentration and adsorbent dose lead to the central point's (i.e., 20 - 40 mg L^{-1} and 3 to 5 g L^{-1}) maximization in percent removal of chromium (VI). The increment in initial Cr (VI) decreases percentage removal of Cr (VI), and the increment of adsorbent dose leads to rise the percentage removal of Cr (VI) until it reaches equilibrium and remains constant. Thus, the peak value of the percentage removal of Cr (VI) for the combined effect of initial concentration and dosage, with values of 40 mg L^{-1} and 5g L^{-1}, respectively, is found to be 96.5%.

Effect of contact time and pH: Figure 4(d) shows the effect of solution pH and adsorption contact time on the percentage removal of Cr (VI) ions by the MAC. From the 3D-interaction plot it can be seen that, with an increase in contact time, the percentage removal of Cr (VI) increases, while the increase in pH causes a decrement in percentage removal. This phenomenon is observed because pH has more effect on the removal efficiency than time. The maximum adsorption efficiency was calculated at a pH value of 1-2. However, for the contact time interval of 10-30 min, there is a rapid increase in adsorption efficiency. The peak value observed at pH 2 and contact time of 30 min is found to be 96.7%.

Effect of pH and initial concentration: The mutual effect of pH and initial concentration on removal efficiency of Cr (VI) at constant dose and adsorption time is demonstrated in Figure 4(e). The removal efficiency decreases with an increase in pH of more than 2 and an initial concentration of more than 40 mg L^{-1}. At a fixed adsorbent dosage and contact time, as the amount of Cr (VI) concentration increases, the percentage of adsorption becomes small. The peak value of removal efficiency for the combined effect of pH and initial concentration of 2 and 40 mg L^{-1}, respectively, was observed to be 96.7 %, alike the other combined effects.

Effect of initial concentration and contact time: The combined effect of contact time and initial adsorbate concentration on the percentage removal of Cr (VI) is shown in Figure 4(f). At small contact time, there will be a higher percentage of Cr (VI) removal due to the protonation of surface functional groups. The maximum value for the percentage removal (96.55 %) is then observed for the intersection of initial concentration and contact time values of 40 mg L^{-1} and 30 min, respectively.

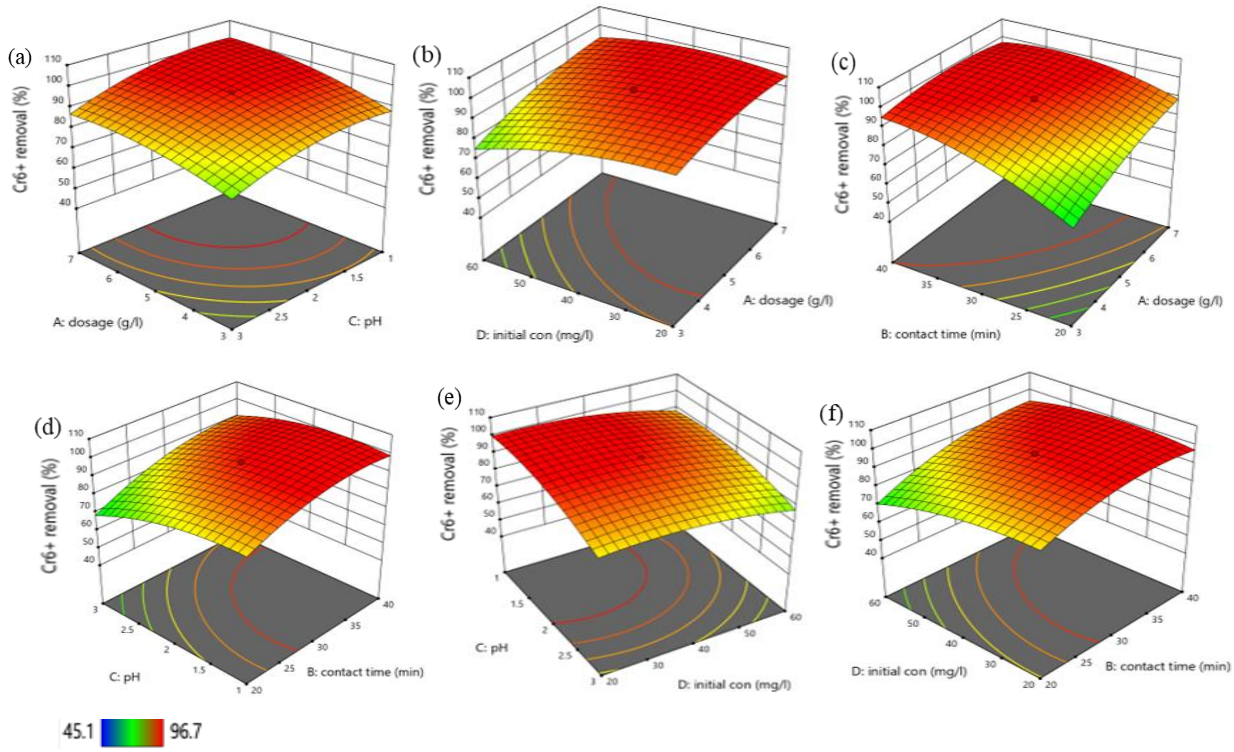

Figure 4: 3D response surface of the combined effects of (a) dosage and contact time, (b) dosage and pH, (c) dosage and initial concentration, (d) contact time and pH, (e) pH and initial concentration, (f) contact time and initial concentration on the removal of Cr (VI) by MAC.

3.2.3. Process optimization and evaluation

Parameter optimization: The criteria showed that pH, adsorbent dose, initial concentration of adsorbent, and contacting time were minimized, by maximizing the amount of Cr (VI) removal efficiency. Optimal conditions are selected and the developed method is subjected to a validation procedure in case it can be used for quantitative purposes. The optimum values found for pH, adsorbent dose, initial concentration of adsorbent, and contacting time was 2, 5 g, 40 mg/L, and 30 min respectively. At the optimum values of the factors given to the software as an input, the percentage removal of Cr (VI) is found to be 96.55%. This value is almost similar to the experimental value obtained as 96% removal efficiency. So that the deviation is less than 1% (0.6 < 1).

ANOVA and model validation: RSM-CCD was applied to model and optimize different process parameters of adsorption capacity of MAC. The yield from design expert RSM-CCD suggested the quadratic model was not aliased and the final empirical mathematical model equation was given in equation (4) in terms of coded factors.

$$Cr(VI)removal = -19.48326 + 16.43911A + 4.53834B + 3.40198C - 0.380557D - 0.260031AB - 0.542188\,AC + 0.069984AD + 0.270063CB + 0.014797BD + 0.085031CD - 0.720130A^2 - 0.059055B^2 - 4.69677C^2 - 0.009554D^2 \quad (4)$$

From the Model summary statistics, it can be seen that, the Predicted R^2 of 0.9355 is in a reasonable agreement with the Adjusted R^2 of 0.9581 (i.e., the difference is less than 0.2) (Figure 5). The adequate precision measures the signal to noise ratio and its value is 25.1389. Hereafter, this model can be used to navigate the design space. The statistical implication of the model was explored by ANOVA. The larger the magnitude of F-test (48.4) and smaller the p – value (< 0.005), the more significant is the corresponding model. All p-value in the model observed was less than 0.0001 enlightening that the model was significant. In this case P-values less than 0.0500 point out model terms are significant. Accordingly, AB, BC, AD, BD, CD, A^2, B^2, C^2, and D^2 are significant model terms. The relationship between actual values and predicted values showed that the actual values are distributed relatively near to the straight line, indicating good fitness of the model (Figure 5). This was an indication of better fitment of the model with the experimental data.

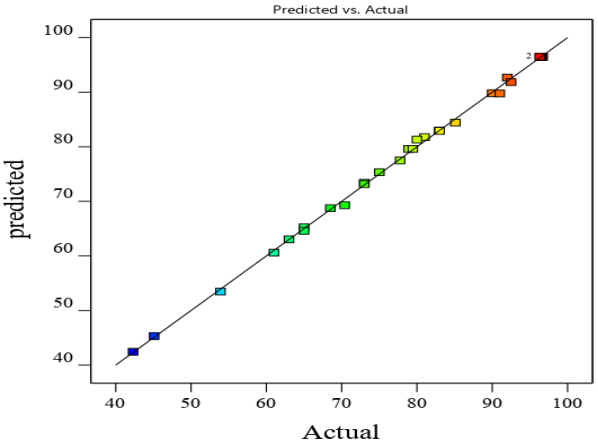

Figure 5: Cr(VI) adsorption removal by MAC showing the actual and predicted value.

3.3. Adsorption isotherm and kinetics

Adsorption Isotherm models: In this study batch adsorption characteristics of Cr (VI) removal by MAC were studied and the results obtained from the experimentation were used to determine the better isotherm model that the adsorption process follows identified such as Langmuir, Freundlich, and Temkin isotherm models [29]. The Langmuir adsorption isotherm is applicable for monolayer adsorption onto a homogeneous surface where as the Freundlich isotherm model assumes that the adsorption process on a heterogeneous surface is in the form of multilayers, where adsorption sites have varied kinship for the adsorbate. As well, in the Temkin isotherm model, the heat of adsorption of adsorbate in a layer decreases linearly with surface coverage due to adsorbent–adsorbate interactions, where the adsorbate adsorption is described by an even distribution of binding energies [30]. From the values of correlation coefficient (R^2) of the three models, Langmuir model for the adsorption of the Cr (VI) was 0.98524, which was slightly lower than the R^2 values of Freundlich model (R^2 = 0.993) and Temkin isotherm (R^2 = 0.996). The results reveal that the adsorption of Cr (VI) on MAC is well fitted to the Temkin model, meaning that MAC surfaces are homogeneous adsorption patches, on which monolayer coverage of Cr (VI) ions were formed on the outer surface. The model's constants and parameters were summarized in Table 3.

Table 3: Summery of adsorption isotherms models for the adsorption of Cr (VI) by MAC

Langmuir isotherm model				**Freundlich isotherm**			**Temkin isotherm**		
R^2	$Q_m(mg\ g^{-1})$	R_L	K_L	R^2	$1/n$	K_F	R^2	B	K_T
0.98524	50.84	0.181	0.089	0.993	0.665	45.40	0.996	10.819	0.87

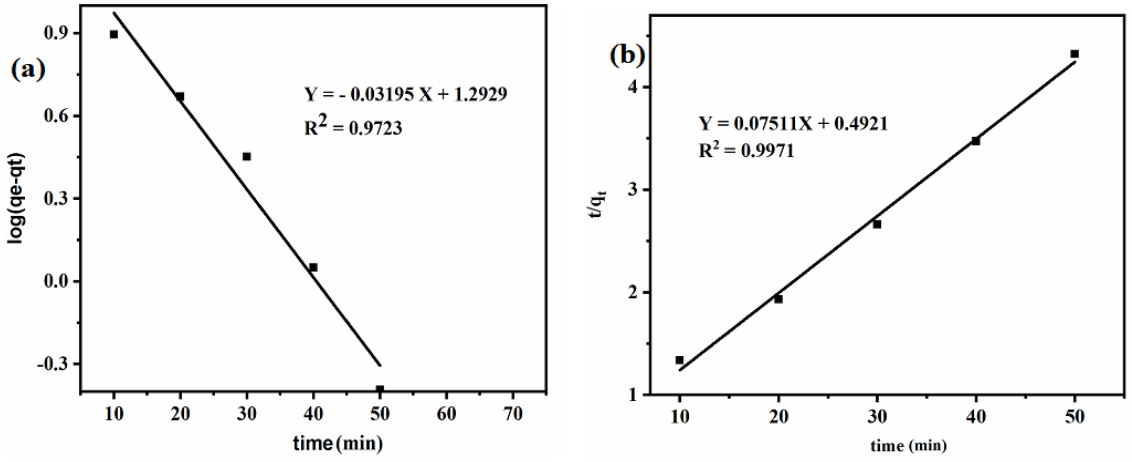

Figure 6: Adsorption kinetics of (a) Pseudo–first order and (b) Pseudo–second order plots.

Adsorption Kinetics study: Pseudo first and second order kinetic models have been verified to fit the data obtained from different adsorption experiments of chromium (VI). The model parameters and rate constants with regression coefficient (R2) values are given in Table 4. The plots (Figure 6 (a & b)) of the kinetic experimental data showed linearity and the R2 values were found to be 0.9722 and 0.99771 for pseudo first and second order kinetics, respectively.

Table 4: Kinetic parameters for first and second-order kinetics.

1st order kinetics			2nd order kinetics		
R^2	q_e	K_1	R^2	q_e	K_2
0.9722	19.62	-0.0735	0.9954	13.31	0.1147

Therefore, from the values of R^2, experimental data is well fitted with pseudo-second order kinetics of adsorption of Cr (VI). It can be noted that rate of the adsorption of Cr (VI) appears to be controlled by the chemisorption.

3.4. Adsorption analysis on real wastewater

Physicochemical Characteristic of real wastewater effluent: The physicochemical characteristics of real wastewater collected from local tannery in Ethiopia was studied. The measured values of BOD, COD, TSS and TDS of the real wastewater were found to be 115 ± 10, 1171.3 ± 104, 1099 ± 6.21 and 2129 ± 76 mg L^{-1}, respectively. However, the recommended maximum permissible amount of BOD, COD, TSS and TDS values are 200, 500, 50 and 2000 mg L^{-1}, respectively [31]. Therefore, the result indicates the poor remediation mechanism employed by the tannery. To assume values of the above parameters within the standard, the real wastewater was treated by using MAC and the BOD, COD, TSS, and TDS

were found to be 41.3 ± 11.8, 317.833 ± 14, 1121.333 ± 19 and 1001.34 ± 9.113 mg L^{-1}, respectively. These values are within the permissible limit of FEPA (Federal Environmental Protection Agency) and EEPA (Ethiopian Environmental Protection Agency) [31]–[33].

Chromium (VI) removal from real wastewater: Before adsorption, the concentration of Cr (VI) in the real wastewater was 2.8437 ± 0.139 ppm. However, after the treatment using MAC, the Cr (VI) concentration was found to be 0.033 ± 0.0054 ppm which is below the allowed value by WHO (i.e., 0.05 ppm of Cr (VI)) [34]. This shows the as prepared MAC has excellent removal efficiency of Cr (VI) from real wastewater. Moreover, the Cr (VI) removal efficiency of our adsorbent material (MAC) was compared with previously reported research works and the MAC we prepared showed the highest Cr (VI) removal efficiency compared to previously reported research works [35]–[37].

3.5. Recycling of MAC Adsorbent

Stablity and recyclablity MAC was conducted and presented in Figure 7 (a & b). The MAC adsorbent was used for five consecutive cycles and for three successive cycles before decreasing its efficiency. The result confirms the excellent stability of the prepared adsorbent. However, its removal efficacy decreased by almost 12% after used for five consecutive cycles. This may be due to the decrease in surface deactivation of MAC during recovery test. Overall, the MAC can be recycled keeping its great adsorption capacity there by making wastewater treatment processes cost effective and sustainable. Moreover, a comparison of the FTIR spectra of MAC before and after batch adsorption indicated the insignificant shifting of individual peaks as shown in Figure 7(b). This result shows that the MAC is stable even after using it for five consecutive adsorption cycles [38].

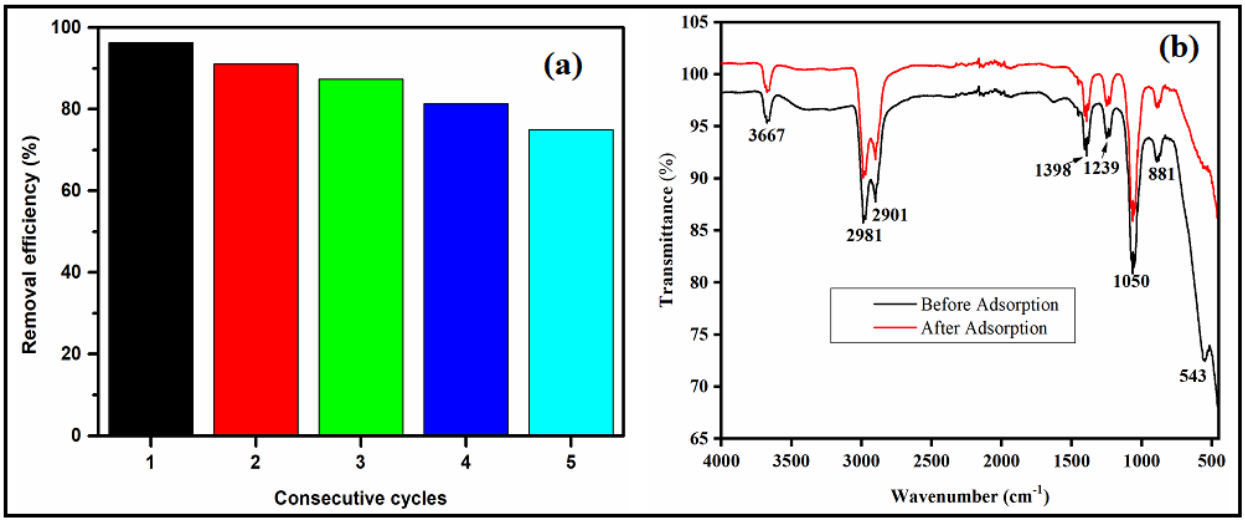

Figure 7: (a) Chromium (VI) removal efficiency of MAC for five consecutive cycles, and (b) FTIR spectra of MAC before and after adsorption of Cr (VI).

4. Conclusions

In this study, magnetic activated carbon (MAC) was synthesized from BSG. The adsorbent was tested and evaluated for removal of Cr (VI) ion aqueous solution using batch adsorption experiment. The synthesized MAC adsorbent was characterized by using BET, FTIR, SEM and XRD. The surface area of MAC adsorbent was 494 m2 g^{-1} with a good morphology as investigated using SEM. The adsorption process were optimized and dosage of 5g L^{-1}, pH of 2, contact time of 30 min and initial concentration of 40 mg L^{-1} were found to be the optimal conditions. The predicted removal of Cr (VI) was 96.55%, which is almost the same with the result obtained under optimum conditions (97.5%). The MAC showed excellent adsorption capacity of 193 mg g^{-1} due to its highest surface area. Furthermore, the adsorption kinetics was best fit to pseudo-second order kinetics model, and adsorption isotherm was best fit to Temkin isotherm with constant value 10.189. Moreover, the MAC shows excellent removal efficiency of Cr (VI) from the real wastewater (from 2.8437 to 0.0333 ppm). The recyclability and stability of the MAC was studied and showed almost the same efficiency for five successive cycles. This result confirms the excellent stability of MAC adsorbent. Therefore, the as-prepared MAC adsorbent can be used for removal of heavy metals from industrials wastewater, specifically to remove Cr (VI) from tannery wastewater.

Conflicts of interest

All authors declare no known conflicts of Interest.

Acknowledgements

All authors are grateful to Addis Ababa Science and Technology University for providing postgraduate research funding and facilities for the research laboratory work.

Author Contributions: Belay Getye- Conceptualization, method development, conducting experiments, data analysis and writing the draft, Tsegaye Sissay Tedla- Resources and data curation, software validation; Gebrehiwot Gebreslassie and Getachew Adam Workneh- Conceptualization, supervision of the experiment, review and editing.

References

[1]. K. M. Dimpe, J. C. Ngila, and P. N. Nomngongo, "Application of waste tyre-based activated carbon for the removal of heavy metals in wastewater," Cogent Eng., vol. 4, no. 1, 2017, doi: 10.1080/23311916.2017.1330912.

[2] M. A. Atieh, "Removal of Phenol from Water Different Types of Carbon – A Comparative Analysis," APCBEE Procedia, vol. 10, pp. 136–141, 2014, doi: 10.1016/j.apcbee.2014.10.031.

[3] E. Altıntıg, et al., "Chemical Engineering Research and Design Effective removal of methylene blue from aqueous solutions using magnetic loaded activated carbon as novel adsorbent," Chem. Eng. Res. Des., vol. 122, pp. 151–163, 2017, doi: 10.1016/j.cherd.2017.03.035.

[4] G. Gebreslassie et al., "Novel g-C3N4/graphene/NiFe2O4 nanocomposites as magnetically separable visible light driven photocatalysts," J. Photochem. Photobiol. A Chem., vol. 382, no. July, p. 111960, 2019, doi: 10.1016/j.jphotochem.2019.111960.

[5] R. Bisht and M. Agarwal, "Methodologies for removal of heavy metal ions from wastewater : an overview Methodologies for removal of heavy metal ions from wastewater : an overview Renu *, Madhu Agarwal and Kailash Singh," Interdiscip. Environ. Rev., vol. 18, pp. 1–20, 2017, doi: 10.1504/IER.2017.10008828.

[6] H. Hu, et al., "A study of heavy metal pollution in China: Current status, pollution-control policies and countermeasures," Sustain., vol. 6, no. 9, pp. 5820–5838, 2014, doi: 10.3390/su6095820.

[7] S. Jiwan and K. A. S, "Effects of Heavy Metals on Soil, Plants, Human Health and Aquatic Life," Int. J. Res. Chem. Environ., vol. 1, pp. 15–21, 2011.

[8] A. E. Burakov et al., "Adsorption of heavy metals on conventional and nanostructured materials for wastewater treatment purposes: A review," Ecotoxicol. Environ. Saf., vol. 148, pp. 702–712, 2018, doi: 10.1016/j.ecoenv.2017.11.034.

[9] S. Mohanty, et al., "Adsorption of Hexavalent Chromium Onto activated carbon," Austin J Biotechnol Bioeng., vol. 1, no. 2, pp. 1–5, 2014.

[10] S. Demcak,et al., "Using of wooden sawdust for copper removal from waters," Nov. Biotechnol. Chim., vol. 18, no. 1, pp. 66–71, 2019, doi: 10.2478/nbec-2019-0009.

[11] Z. J. Harandi, et al., "Synthesis and characterisation of magnetic activated carbon / diopside nanocomposite for removal of reactive dyes from aqueous solutions : experimental design and optimisation," Int. J. Environ. Anal. Chem., vol. 00, pp. 1–27, 2019, doi: 10.1080/03067319.2019.1597867.

[12] K. S. Obayomi et al., "Development of low-cost bio-adsorbent from agricultural waste composite for Pb (II) and As (III) sorption from aqueous solution Development of low-cost bio-adsorbent from agricultural waste composite for Pb (II) and As (III) sorption from aqueous," Cogent Eng., vol. 6, pp. 1–17, 2019, doi: 10.1080/23311916.2019.1687274.

[13] Parlayıcı and E. Pehlivan, "Removal of metals by Fe3O4 loaded activated carbon prepared from plum stone (Prunus nigra): Kinetics and modelling study," Powder Technol., vol. 317, pp. 23–30, 2017, doi: 10.1016/j.powtec.2017.04.021.

[14] C. Anyika, et al., "Synthesis and characterization of magnetic activated carbon developed from palm kernel shells," Nanotechnol. Environ. Eng., vol. 2, no. 1, p. 16, Dec. 2017, doi: 10.1007/s41204-017-0027-6.

[15] E. Kassahun, et al., "The Application of the Activated Carbon from Cordia africana Leaves for Adsorption of Chromium (III) from an Aqueous Solution," J. Chem., vol. 2022, pp. 1–11, Nov. 2022, doi: 10.1155/2022/4874502.

[16] T. T. Nadew, et al., "Synthesis of activated carbon from banana peels for dye removal of an aqueous solution in textile industries: optimization, kinetics, and isotherm aspects," Water Pract. Technol., vol. 18, no. 4, pp. 947–966, Apr. 2023, doi: 10.2166/wpt.2023.042.

[17] A. Turki, et al, , "Infrared Spectra for Alfa Fibers Treated with Thymol," J. Glycobiol., vol. 07, no. 01, pp. 1–8, 2018, doi: 10.4172/2168-958x.1000130.

[18] B. Sadhukhan, et al., "Optimisation using central composite design (CCD) and the desirability function for sorption of methylene blue from aqueous solution onto Lemna major," Karbala Int. J. Mod. Sci., vol. 2, no. 3, pp. 145–155, 2016, doi: 10.1016/j.kijoms.2016.03.005.

[19] S. Kumar, et al., "Application of response surface methodology (RSM) for optimization of leaching parameters for ash reduction from low-grade coal," Int. J. Min. Sci. Technol., vol. 28, no. 4, pp. 621–629, 2018, doi: https://doi.org/10.1016/j.ijmst.2018.04.014.

[20] K. K. Onchoke and S. A. Sasu, "Determination of Hexavalent Chromium (Cr(VI)) Concentrations via Ion Chromatography and UV-Vis Spectrophotometry in Samples Collected from Nacogdoches Wastewater Treatment Plant, East Texas (USA)," Adv. Environ. Chem., vol. 2016, no. Iii, pp. 1–10, Feb. 2016, doi: 10.1155/2016/3468635.

[21] Saruchi Puri and V. Kumar, "Adsorption kinetics and isotherms for the removal of rhodamine B dye and Pb +2 ions from aqueous solutions by a hybrid ion-exchanger," Arab. J. Chem., vol. 12, no. 3, pp. 316–329, 2019, doi: 10.1016/j.arabjc.2016.11.009.

[22] A. A. Attia, et al., "Adsorption of chromium ion (VI) by acid activated carbon," Brazilian J. Chem. Eng., vol. 27, no. 1, pp. 183–193, 2010, doi: 10.1590/S0104-66322010000100016.

[23] T. Dula, et al., "Adsorption of Hexavalent Chromium from Aqueous Soluti on Using Chemically Activated Carbon Prepared from Locally Available Waste of Bamboo (Oxytenanthera abyssinica)," Environ. Chem., pp. 1–10, 2014.

[24] B. Y. Yu and S. Y. Kwak, "Assembly of magnetite nanocrystals into spherical mesoporous aggregates with a 3-D wormhole-like pore structure," J. Mater. Chem., vol. 20, no. 38, pp. 8320–8328, 2010, doi: 10.1039/c0jm01274b.

[25] S. Gholamiyan, et al., "RSM optimized adsorptive removal of erythromycin using magnetic activated carbon: Adsorption isotherm, kinetic modeling and thermodynamic studies," Sustain. Chem. Pharm., vol. 17, no. September, p. 100309, 2020, doi: 10.1016/j.scp.2020.100309.

[26] N. Belachew and H. Hinsene, "Preparation of cationic surfactant-modified kaolin for enhanced adsorption of hexavalent chromium from aqueous solution," Appl. Water Sci., vol. 10, no. 1, p. 38, Jan. 2020, doi: 10.1007/s13201-019-1121-7.

[27] S. A. Saafan, et al., "FTIR, DC, and AC electrical measurements of Mg Zn Nano-ferrites and their composites with Polybenzoxazine," Appl. Phys. A, vol. 127, no. 10, p. 800, Oct. 2021, doi: 10.1007/s00339-021-04947-2.

[28] T. Altun, "Cr (VI) removal using Fe 2 O 3 -chitosan-cherry kernel shell pyrolytic charcoal composite beads," Environ. Eng. Res, vol. 25, pp. 426–438, 2020.

[29] B. Choudhary and D. Paul, "Isotherms, kinetics and thermodynamics of hexavalent chromium removal using biochar," J. Environ. Chem. Eng., vol. 6, no. 2, pp. 2335–2343, 2018, doi: 10.1016/j.jece.2018.03.028.

[30] R. Wahab, et al., "Photocatalytic TMO-NMs adsorbent: Temperature-Time dependent Safranine degradation, sorption study validated under optimized effective equilibrium models parameter with standardized statistical analysis," Sci. Rep., vol. 7, no. January, pp. 1–15, 2017, doi: 10.1038/srep42509.

[31] H. R. Amanial, "Physico-chemical characterization of tannery effluent and its impact on the nearby river," J. Environ. Chem. Ecotoxicol., vol. 8, no. 6, pp. 44–50, 2016, doi: 10.5897/jece2015.0365.

[32] T. N. Chikwe and M. C. Onojake, "An appraisal of physicochemical parameters and some trace metals at the disposal points of five industrial effluents in Trans-Amadi Industrial Area of Port Harcourt, Nigeria," J. Appl. Sci. Environ. Manag., vol. 21, no. 1, pp. 31–37, 2017, doi: 10.4314/jasem.v21i1.4.

[33] R. Bhateria and D. Jain, “Water quality assessment of lake water: a review,” Sustain. Water Resour. Manag.,vol. 2, no. 2, pp. 161–173, 2016, doi: 10.1007/s40899-015-0014-7.

[34] S. T. Ametepey, et al., “Health risk assessment and heavy metal contamination levels in vegetables from Tamale Metropolis, Ghana,” Int. J. Food Contam., vol. 5, no. 1, p. 5, Dec. 2018, doi: 10.1186/s40550-018-0067-0.

[35] K. C. Khulbe and T. Matsuura, “Removal of heavy metals and pollutants by membrane adsorption techniques,” Appl. Water Sci., vol. 8, no. 1, p. 19, Mar. 2018, doi: 10.1007/s13201-018-0661-6.

[36] G. Arslan, et al., “Hexavalent chromium removal by magnetic particle-loaded micro-sized chitinous egg shells isolated from ephippia of water flea,” Int. J. Biol. Macromol., vol. 129, pp. 23–30, 2019, doi: 10.1016/j.ijbiomac.2019.01.180.

[37] S. Nethaji, et al., “Preparation and characterization of corn cob activated carbon coated with nano-sized magnetite particles for the removal of Cr(VI),” Bioresour. Technol., vol. 134, pp. 94–100, 2013, doi: 10.1016/j.biortech.2013.02.012.

[38] N. T. Abdel-Ghani, et al., “Magnetic activated carbon nanocomposite from Nigella sativa L. waste (MNSA) for the removal of Coomassie brilliant blue dye from aqueous solution: Statistical design of experiments for optimization of the adsorption conditions,” J. Adv. Res., vol. 17, pp. 55–63, 2019, doi: 10.1016/j.jare.2018.12.004.